Spatial Correlation Analysis of the Pharmacological Conversion of Sustained Atrial Fibrillation in Conscious Goats by Cibenzoline

B.P.T. Hoekstra[1], C.G.H. Diks[2], M.A. Allessie[3] and J. DeGoede[4]

Archives of Physiology and Biochemistry 2000, Vol. 108, No. 4, 332–348

[1]Division of Image Processing, Department of Radiology, Leiden University Medical Center, The Netherlands
[2]Center for Nonlinear Dynamics in Economics and Finance, Department of Economics and Econometrics, University of Amsterdam, The Netherlands
[3]Cardiovascular Research Institute Maastricht, Department of Physiology, Maastricht University, The Netherlands
[4]Department of Physiology, University of Leiden, The Netherlands

Address: B.P.T. Hoekstra, Leiden University Medical Center, Division of Image Processing, Department of Radiology, P.O. Box 9600, 2300 RC Leiden, The Netherlands. Tel: +31–71–526 2137; Fax: +31–71–526 6801; Email: B.P.T.Hoekstra@lumc.nl

ABSTRACT

The nonlinear spatial redundancy and the linear spatial correlation function were used to investigate to what extent nonlinearity was involved in the coupling of atrial regions and how organization in activation patterns of sustained atrial fibrillation (AF) had been modified by administration of the class IC agent cibenzoline in the experimental model of sustained AF in instrumented conscious goats.

Electrograms were measured in five goats during sustained AF and when the fibrillation interval had been prolonged to about 25%, 50% and 85% (CIB25, CIB50, CIB85) with respect to control. The nonlinear association length and linear correlation length were estimated along the principle axes of two–dimensional correlation maps estimated from the spatial redundancy and the spatial correlation function, respectively.

The estimated short axis association length in the right atrium increased already shortly after the start of infusion (CIB25, +61%), and remained significantly different from control during the experiment, including the effects of non–simultaneous interaction. At CIB85 the association length had almost become twice as long with respect to control (increase from 16 to 29 mm, +89%), while in the left atrium changes were less pronounced (increase from 9 to 12 mm, +32%). The linearized association length which was estimated using multivariate surrogate data increased more gradually and was less sensitive to changes in spatial organization. The results of the spatial correlation analysis suggest that the drug–induced nonlinearity in the spatio–temporal dynamics of sustained AF is related to activation patterns which are characterized by extended uniformly propagating fibrillation wavefronts (AF type I).

We conclude that cibenzoline enhanced the spatial organization of sustained AF associated with a transition from type II to type I AF activation patterns. This may destabilize the perpetuation of AF since an increase in association length is equivalent to a reduction of atrial tissue mass available to support reentrant circuits. The results are consistent with the hypothesis that larger association lengths result from fewer and larger reentrant circuits. It is argued that effects of diminished curvature of fibrillation wavefronts are anti–arrhythmic under conditions of suppressed excitability imposed by cibenzoline. Termination of AF may be mediated by a mechanism resembling a bifurcation of the dynamics which sets in when the ends of fractionated wavefronts cannot sufficiently curve anymore to maintain a positive balance of newly generated wavelets needed to sustain AF.

KEYWORDS: spatial organization, cross correlation, cross redundancy, correlation length, association length, atrial fibrillation, anti–arrhythmic drugs, cibenzoline, cardioversion

INTRODUCTION

In this paper the changes in spatial organization during pharmacological conversion of sustained AF are characterized and quantified. Data were obtained from electrophysiological experiments to terminate AF by infusion of the class IC anti–arrhythmic drug cibenzoline. Multiple atrial epicardial electrograms were recorded in instrumented conscious goats, in which sustained AF had been electrically induced by continuous maintenance of AF using an automatic fibrillation pacemaker (Wijffels et al., 1995). Maintaining the high rate of AF induced electrophysiological changes in otherwise healthy atria (pacing induced electrical remodeling) which may change the action of anti–fibrillatory drugs. For instance, the success rate of pharmacological cardioversion significantly decreases when AF is allowed to persist over a longer period of time. It is also known from clinical studies that the arrhythmia, once it is present as paroxysmal AF, finally becomes permanent after a variable amount of time (domestication of atrial fibrillation). Thus, electrical remodeling as observed in the experimental model of sustained AF in goats (Allessie, 1998) may be an interesting novel target for therapy of AF and it is important to test the effects of pharmacological intervention in a model of *chronic* AF.

Hoekstra et al. (2000) applied correlation measures to assess the degree of spatial complexity in atrial activation patterns during sustained AF. Since an alteration of the spatial organization may lead to termination of AF, it is interesting to track changes in the correlation length during chemical conversion of AF. In the present study the nonlinear redundancy and the linear correlation function were used to investigate to what extent nonlinearity was involved in the coupling of atrial regions and how organization in activation patterns of sustained AF had been modified by administration of cibenzoline in the goat model of chronic AF.

MATERIALS AND METHODS

Data Acquisition and Selection

The data acquisition and selection of electrograms for the spatial correlation analysis has previously been described in detail (Hoekstra et al., 2000). In this study, sets of fifteen electrograms were recorded simultaneously from both the left and right atrial free wall from the same five goats. Far field ventricular contributions were removed from atrial electrograms by a coherent averaging procedure prior to the correlation analysis.

Data were selected according to a protocol described elsewhere (Hoekstra et al., 1997), in which a nonlinear analysis was performed on local atrial epicardial electrograms to characterize the dynamics of sustained AF during pharmacological conversion with cibenzoline. Briefly, cibenzoline (Cipralan®, Searle, Belgium) was administered by intravenous infusion (rate 0.1 $mg{\cdot}kg^{-1}{\cdot}min^{-1}$) causing a dose dependent increase in the mean AF interval. Electrograms were measured during sustained AF (control) and when the AF interval had been prolonged to about 25%, 50% and 85% with respect to control. These episodes are referred to as CIB25, CIB50 and CIB85 hereafter.

Spatial Correlation Measures

Hoekstra et al. (2000) applied spatial correlation measures to characterize activation patterns of sustained AF. These measures are used here to quantify the changes in atrial activation after administration of cibenzoline. Spatial correlation maps were constructed from the linear correlation function and the nonlinear redundancy and we distinguished correlation resulting from interaction of simultaneous events (delay $\tau = 0$, no relative time shift between sites) from correlation resulting from interaction taking place between non–simultaneous events (delay $\tau = \tau_{\max}$, corresponding to the maximum correlation value). The latter type of correlation accounts for similar electrical activity recorded at different atrial sites yet occurring at a different time. In this way spatial coupling introduced by propagation of fibrillation wavelets was incorporated in the correlation measures. It is important to account for wave propagation, since AF is maintained by fibrillation waves which wander through the atria before they extinguish, fuse or collide with other wavelets.

Iso–correlation contours were drawn in the correlation maps at levels $e^{-\frac{1}{4}}$, $e^{-\frac{1}{2}}$, e^{-1}, e^{-2}, e^{-4} with respect to the maximum correlation to visualize the decay of spatial correlation. It was observed by Hoekstra et al. (2000) that the structure of spatial organization in correlation maps of sustained AF was in general not circular, but iso–correlation contours were elongated and elliptically shaped. Therefore spatial correlation was characterized in the two principal directions of the maps. To this end the set of correlation values was first rotated and put onto main axes using singular value decomposition. Next, the decay of spatial correlation was fitted with an exponential function in the direction of the short and long principal axis of the rotated correlation map. The linear correlation length was defined as the space constant determined from the decay along the short axis correlation curve of the measure C_0 or C_{m}. Subscripts indicate a relative time shift $\tau = 0$ and $\tau = \tau_{\max}$ (delay corresponding to the maximum value of the correlation measure) between electrograms, respectively. The nonlinear measure, termed association length, was obtained from the decay along the short axis of the spatial redundancy I_0 or I_{m}.

The cross correlation and the redundancy are two different quantities and only a qualitative comparison of these measures is appropriate. Hence, the method of multivariate surrogate data was applied for a quantitative comparison of the linear and nonlinear correlation measures (Hoekstra et al., 2000). Briefly, surrogate electrograms were generated which are realizations of a stochastic process but contain the same linear characteristics as the measured data. For example, statistics such as the linear auto– and cross correlation of the electrograms are preserved. Also, a rescaling was applied to the surrogate electrograms to restore the measured amplitude distribution. However, nonlinearities contained in the original electrograms had been destroyed since the phases of each of the measured time series were randomized separately. The method of surrogate data consists of comparing a nonlinear statistic, in this case the association length, for both the measured and the surrogate dataset. To this end correlation maps were also constructed for the linearized spatial redundancy estimated from the surrogate electrograms. Next, the association length estimated from the linearized spatial redundancy was compared to the association length estimated from the spatial redundancy of the measured electrograms.

If substantial differences are found, the hypothesis that the spatial organization observed in activation patterns of AF was generated by a linear random process can be rejected.

Statistical Analysis

Two–way analysis of variance was applied (SAS software package, the SAS Institute Inc., USA) to test for equivalence of association length, with goats and drug dose as factors. Bonferroni's t test was used to compare the estimated values at different dose of cibenzoline. A probability value $p < 0.05$ was considered to be statistically significant.

RESULTS

In the next sections we present the results of the spatial correlation analysis applied to coherent averaged epicardial atrial electrograms after the electrophysiological substrate of AF had been modified with cibenzoline. Visual inspection of the recorded time series revealed that many electrograms consisted of discrete activation complexes most of the time without a large degree of fragmentation. This means that activation was locally fairly homogeneous during AF, and that many sites were activated by uniformly conducting wavelets. Therefore, we will first present an example of uniformly propagating activation waves during sustained AF after modification by cibenzoline. It will also serve to illustrate features of the AF dynamics which distinguish linear from nonlinear aspects of spatial correlation.

Uniform Wave Propagation during Atrial Fibrillation

An episode of sustained AF was selected in which the mean fibrillation interval had been prolonged from 96 to 178 ms by administering cibenzoline (CIB85, goat no. 2). Fig. 1 (left panel) shows coherent averaged right atrial electrograms RA_0 to RA_{24} recorded from a line of four electrodes (separation 8 mm).

The reference electrogram RA_0 is shown at the top, and the direction of activation is indicated with an arrow. The cleaned (i.e. coherent averaged) electrograms show discrete activation complexes characterisic for uniform conduction and this episode was characterized by broad activation waves which propagated along the line of electrodes. In Fig. 1 (right panel) surrogate electrograms are shown which were constructed from the cleaned electrograms. Although each surrogate electrogram is a realization of a random process, the coupling between the electrograms was not altogether lost since linear cross correlation between the signals was kept intact. Thus, the aspect of wave propagation was still present in the surrogate dataset, which is also evident from a visual inspection of the phase relation between the surrogate electrograms (Fig. 1, right panel).

Fig. 2 shows the results of the correlation analysis for the electrograms shown in Fig 1. Each curve shows the temporal correlation as a function of the relative time shift τ between two electrodes. Different curves correspond to the temporal correlation measures estimated from electrograms RA_0, RA_8, RA_{16} and RA_{24} recorded at distances 0 (viz. autocorrelation), 8, 16 and 24 mm from the reference RA_0, respectively. The linear and nonlinear spatial correlation

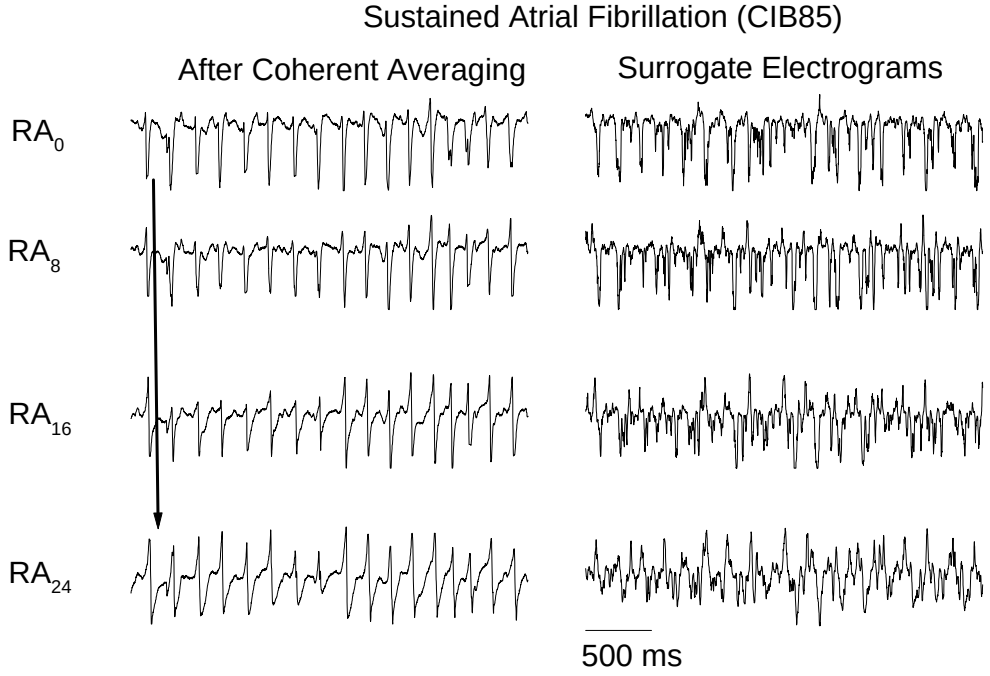

Figure 1: Left panel: Four cleaned right atrial epicardial electrograms $\mathrm{RA}_0 \ldots \mathrm{RA}_{24}$ recorded from a row of electrodes (separation 8 mm) during sustained atrial fibrillation (goat no. 2). The mean fibrillation interval had been prolonged to 178 ms by infusion of cibenzoline. Right panel: Surrogate electrograms were constructed from the electrograms shown in the left panel by preserving the linear auto– and cross correlations of the signals, while the phase in each electrogram was randomized. Each surrogate electrogram was given the original amplitude distribution.

measures were determined from these curves by tabulating the values at delays $\tau = 0$ and $\tau = \tau_{\max}$ as a function of the distance to the reference electrode. The decrease of temporal correlation with increasing distance (Fig. 2, indicated by arrows) reflects the loss of spatial coupling.

I_0 (upper left panel) at 24 mm from the reference site decreased to a level of about e^{-1} of the maximum redundancy. For increasing electrode distance I_{m} corresponded to the peak value located at a delay $\tau_{\max}$ corresponding to the conduction time the activation waves needed to travel the distance between the electrodes. At a distance of 24 mm from the reference site, the delay was equal to $\tau_{\max} = 42$ ms. Assuming uniform conduction along the line of electrodes, the velocity of propagating waves was estimated as approximately $\frac{24}{42}$ mm $\cdot$ ms $^{-1} = 57$ cm $\cdot$ s^{-1}. In this case the lag $\tau_{\max}$ was positive so that, by convention, the electrical activity at the reference site was delayed with respect to activation recorded at the other electrodes. This was consistent with the direction of the propagating activation waves (Fig. 1, indicated by an arrow). Smaller peaks in the temporal correlation appeared to the left and right of the peak at $\tau_{\max}$ because of the temporal periodicity in the atrial electrograms. The distance from each of the side peaks to the peak I_{m} corresponded to the mean fibrillation interval during this episode of AF.

The redundancy calculated for the surrogate data (lower left panel) also showed a peak located at a shift equal to the conduction delay along the row of electrodes. However, the

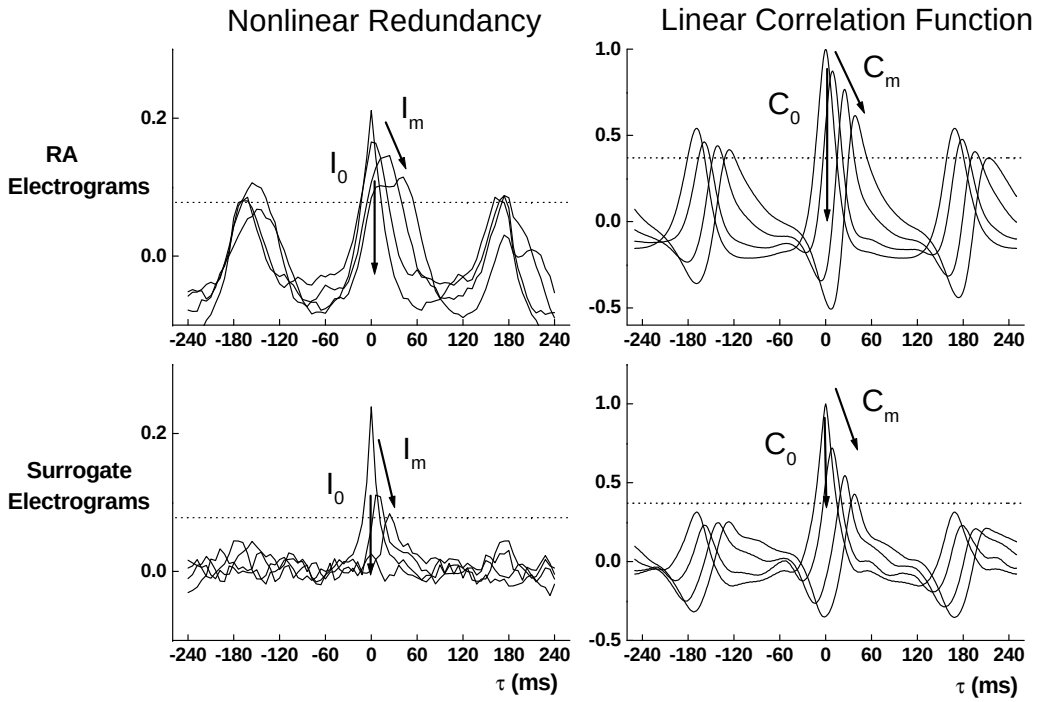

Figure 2: Example of the spatial correlation measures estimated from the right atrial (RA) electrograms shown in Fig. 1. Different curves (as a function of time shift τ) correspond to the correlation estimated from electrograms at distances 0 (viz. autocorrelation), 8 (RA_8), 16 (RA_{16}) and 24 mm (RA_{24}) with respect to the reference electrogram (RA_0). Left column: the nonlinear redundancy I_0 and I_m estimated from the original and surrogate electrograms (top and bottom panels, respectively). The spatial decay of correlation with increasing electrode distance is indicated by arrows. Right column: the linear correlation functions C_0 and C_m estimated from the same dataset. The e^{-1} level (37% of the maximum correlation value) is indicated by a dashed line. The resolution of the linear and nonlinear correlation measures along the τ axis was 1 and 6 ms, respectively. See text for further description. Note that, since $q = 2$, I_0 and I_m may be negative (Pompe, 1993)

peak values I_m were considerably smaller than the values estimated from the original activation waves. Secondly, the positive values of I_0 which persisted for increasing electrode distance in the original redundancy had disappeared in the linearized redundancy. From these qualitative differences between the redundancy calculated for the original data and their surrogates, we conclude that in this example nonlinearity is present in the spatio–temporal dynamics of AF through the presence of extended, uniformly conducting fibrillation waves.

The linear correlation function C_0 (upper right panel) rapidly declined with increasing distance, reaching significant negative values. The maximum value C_m was located at a delay $\tau_{max} = 39$ ms at 24 mm from the reference site, which is consistent with the location of the corresponding maximum I_m for the spatial redundancy. The linear correlation curves calculated for the surrogate data (lower right panel) were very similar to those of the original data. This is to be expected since the surrogate data should mimick the linear properties of the original data and may be considered as a consistency check for the construction of the surrogate data.

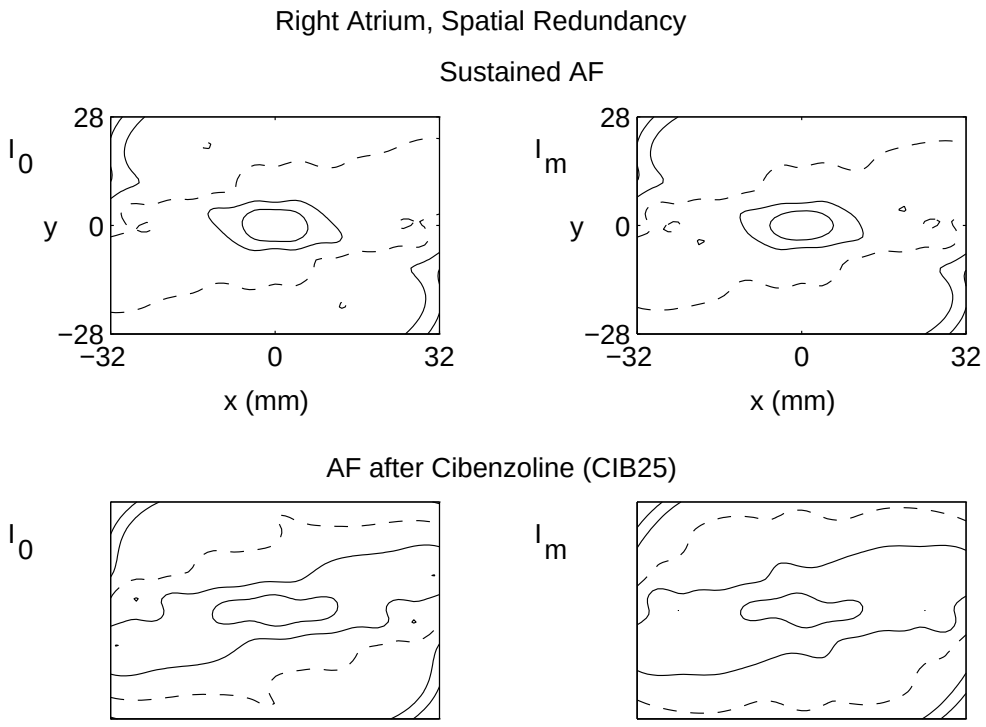

Figure 3: Right atrial correlation maps of the spatial redundancy I_0 (left column) and I_m (right column) during sustained atrial fibrillation (AF) and shortly after infusion of cibenzoline (CIB25). The short axis correlation length of the e^{-1} contour increased from 15.9 during control to 19.9 mm (I_0) and 24.3 mm (I_m) after administration of cibenzoline.

Analysis of Right Atrial Activation Patterns

In the previous section features of the different correlation measures were illustrated using an example of uniformly propagating fibrillation waves along a line of electrodes. We will now proceed with the analysis of the two–dimensional AF activation pattern measured by the electrode matrix. The various correlation measures are discussed by means of a representative example (goat no. 3). The e^{-1} iso–correlation contour served as a reference in the different types of correlation maps, and its short and long principle axis are referred to as the short and long axis, respectively, hereafter. For the sake of a concise graphical presentation, only the correlation maps of CIB25 and sustained AF (control) are shown.

In the right atrium, the short axis length of the spatial redundancy I_0 (Fig. 3, left column) first increased from 15.9 mm during sustained AF to 19.9 mm (CIB25), and then decreased again to 16.0 and 15.0 mm during CIB50 and CIB85, respectively. The e^{-1} contours were stretched, so that the long axis exceeded the border of the electrode matrix throughout the experiment. In correlation maps of I_m (Fig. 3, right column) the short axis length progressively increased from 15.9 mm to 24.3 mm (CIB25), and exceeded the border of the electrode matrix at CIB50 and CIB85. The long axis length exceeded the border of the electrode matrix during the experiment.

In Fig. 4, right atrial correlation maps are shown of the linearized spatial redundancy estimated from a set of surrogate electrograms. The length of the short axis of the linearized redundancy I_0 hardly increased in the course of the experiment (range 6–8 mm). The long axis length increased from 15.8 mm (sustained AF) and exceeded the border of the electrode

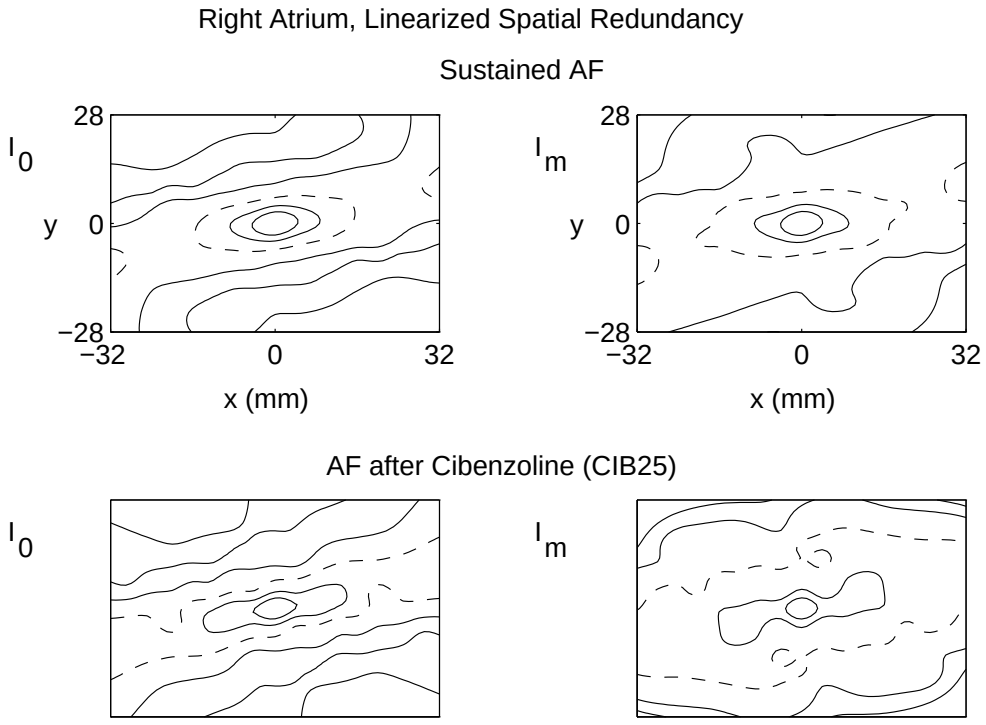

Figure 4: Right atrial correlation maps of the linearized spatial redundancy I_0 (left column) and I_m (right column) during sustained atrial fibrillation (AF) and shortly after infusion of cibenzoline (CIB25). The short axis correlation length of the e^{-1} contour (6.6 mm) estimated from I_0 hardly increased, while an increase from 8.2 to 11.2 mm was observed for I_m after infusion of cibenzoline.

matrix shortly after cibenzoline had been infused. Comparing the correlation maps $I_0[o]$ and $I_0[s]$ ($[o]$ referring to the original and $[s]$ to the surrogate electrograms), the short axis length of $I_0[o]$ was larger than estimated from $I_0[s]$ during sustained AF as well as during infusion of cibenzoline (Fig. 3 and 4, left column). Correlation maps of the linearized redundancy $I_\mathrm{m}[s]$ are shown in Fig. 4 (right column). The short axis length was 8.2 mm during control, 11.2 mm at CIB25 and further increased to 13.8 mm at CIB85. Thus in the right atrium, also the short axis length in correlation maps of $I_\mathrm{m}[o]$ was substantially larger than in maps of $I_\mathrm{m}[s]$. The long axis length estimated from $I_\mathrm{m}[o]$ was 20.7 mm during control and exceeded the border of the electrode matrix shortly after cibenzoline had been administered.

Right atrial correlation maps of the spatial correlation function C_0 (Fig. 5, left column) showed elongated contours which kept the same orientation throughout the experiment. The long axis length exceeded the border of the mapped area and the short axis length slightly increased from 11.2 mm (control) to 14.4 mm at CIB85. Contours in correlation maps of C_m (Fig. 5, right column) had widened with respect to C_0 and spatial correlation was decaying more slowly, since effects of wave propagation were incorporated in C_m. In the right atrium, the short axis length increased from 23.5 mm to a value exceeding the border of the mapped area and the e^{-1} contour covered the entire correlation map shortly after cibenzoline had been administered (CIB25).

Table 1 displays the average association length estimated from an exponential fit of the

	SAF		CIB25		CIB50		CIB85	
	LA	RA	LA	RA	LA	RA	LA	RA
$I_0[o]$:	8.2 (3.6)	15.2 (5.9)	7.5 (1.7)	21.8 (11.2)	7.2 (1.7)	19.9 (7.7)	8.1 (0.3)	20.7 (9.5)
			-9%	43%	-12%	31%	-1%	36%
$I_0[s]$:	5.1 (1.6)	5.5 (0.9)	5.2 (1.6)	5.9 (1.1)	5.8 (0.8)	6.2 (1.4)	6.4 (1.1)	7.5 (2.2)
			2%	7%	14%	13%	26%	36%*
$I_m[o]$:	9.2 (4.1)	15.5 (5.5)	8.9 (1.7)	25.0 (9.7)	12.1 (6.4)	27.3 (9.8)	12.1 (2.4)	29.3 (8.1)
			-3%	61%*	32%	76%*	32%	89%*
$I_m[s]$:	6.4 (2.3)	9.4 (3.6)	6.6 (1.1)	11.6 (4.4)	8.4 (2.9)	12.6 (3.9)	8.3 (1.1)	13.8 (3.9)
			3%	23%*	31%	34%*	30%	47%*

Table 1: Association length (mm) estimated from an exponential fit of the short principal axis of the spatial redundancy I_0 and I_m. Symbols $[o]$ and $[s]$ refer to the original and linearized redundancy, respectively. SAF indicates sustained atrial fibrillation; CIB25, CIB50, CIB85, atrial fibrillation during infusion of cibenzoline; LA, left atrium; RA, right atrium; Results are presented as Mean (SD), the percentage shown indicates the mean relative change in association length with respect to SAF. Coherent averaging of far-field ventricular potentials was applied in episodes of atrial fibrillation. *, $p < 0.05$ with respect to control.

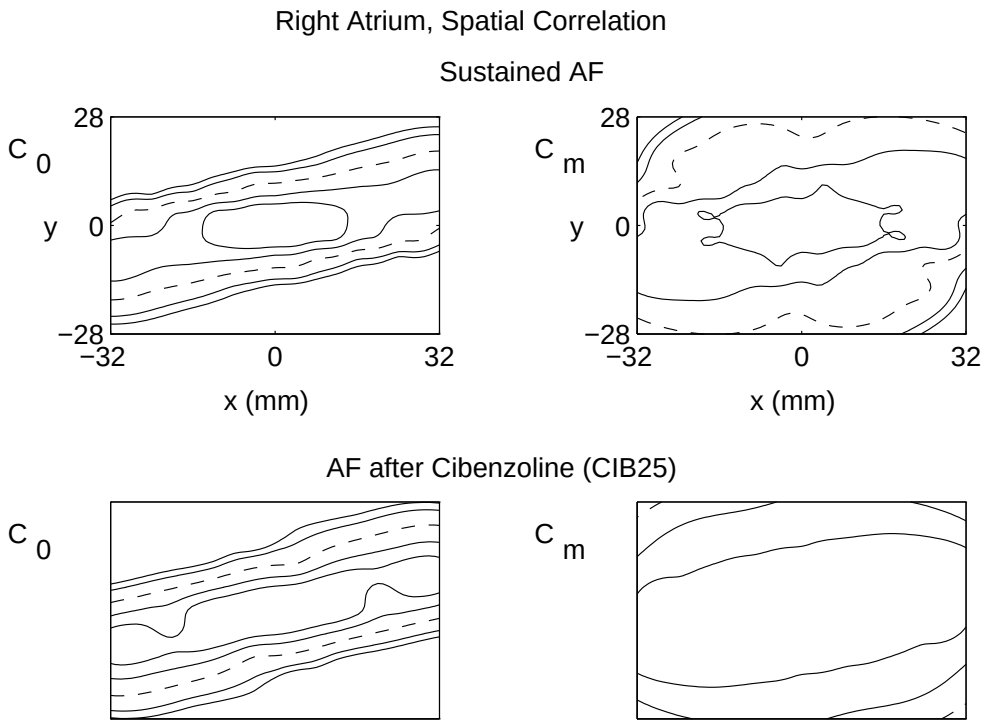

Figure 5: Right atrial correlation maps of the spatial correlation C_0 (left column) and C_{m} (right column) during sustained atrial fibrillation (AF) and shortly after infusion of cibenzoline (CIB25). The short axis correlation length of the e^{-1} contour (11.2 mm) estimated from C_0 did not noticably increase while for C_{m} the correlation length increased from 23.5 mm to a value which exceeded the border of the mapped area shortly after administration of cibenzoline.

short principal axis of the spatial redundancies for the entire population of five goats. In the right atrium, the association length estimated from $I_0[o]$ increased from 15.2 ± 5.9 mm during control to 21.8 ± 11.2 mm after infusion of cibenzoline (CIB25, +43%), and did not change much thereafter. For the linearized redundancy $I_0[s]$, a small increase in association length was observed from 5.5 ± 0.9 cm to 7.5 ± 2.2 mm (CIB85, +36%). The association length estimated from $I_{\mathrm{m}}[o]$ changed from 15.5 ± 5.5 mm (sustained AF) to 25.0 ± 9.7 mm shortly after the start of infusion of cibenzoline (CIB25, +61%) and further increased to 29.3 ± 8.1 mm (+89%) at the highest dose of cibenzoline. The linearized redundancy $I_{\mathrm{m}}[s]$ showed a progressive increase from 9.4 ± 3.6 mm during control to 13.8 ± 3.9 mm (CIB85, +47%) with a relative prolongation of 23% shortly after the start of drug infusion (CIB25).

Analysis of variance showed a significant increase in association length for both $I_{\mathrm{m}}[o]$ and $I_{\mathrm{m}}[s]$ in the right atrium during infusion of cibenzoline (Table 1). No significant differences were found for I_0, except for the linearized redundandy $I_0[s]$ during CIB85 in the right atrium.

Analysis of Left Atrial Activation Patterns

The left atrial correlation maps of the spatial redundancy I_0 are shown in Fig. 6 (left column).

The short axis length slightly decreased from 10.7 mm during control to 8.6 mm after infusion of cibenzoline (CIB25-85). Iso–correlation contours were elliptically shaped and the long axis length increased from 21.3 mm during sustained AF to 30.6 mm (CIB25), 23.8 mm (CIB50)

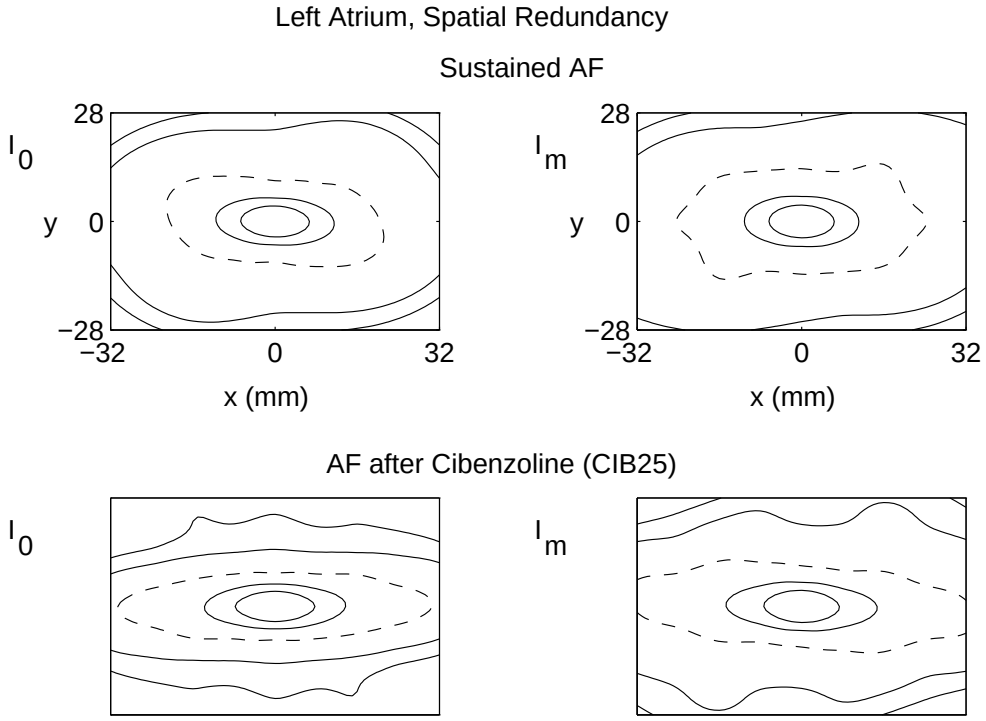

Figure 6: Left atrial correlation maps of the spatial redundancy I_0 (left column) and I_m (right column) during sustained atrial fibrillation (AF) and shortly after infusion of cibenzoline (CIB25). The short axis correlation length of the e^{-1} contour slightly decreased from 10.7 to 8.6 mm (I_0) and from 13.7 to 10.4 mm (I_m) after administration of cibenzoline. The long axis lengths increased from 21.3 and 23.5 mm, respectively, to a value about equal to the extension of the mapped region (32 mm).

and 26.8 mm (CIB85). In correlation maps of I_m (Fig. 6, right column), the short and long axis length was only slightly larger than estimated from I_0. The short axis length decreased from 13.7 mm during sustained AF to 9.9 mm at CIB85, while the long axis length was 23.5 mm (control) and increased to 31.3 mm during CIB85.

Fig. 7 (left column) shows left atrial correlation maps of the linearized redundancy $I_0[s]$. It was observed that during sustained AF the short axis length of the redundancy $I_0[o]$ was somewhat larger (10.7 versus 7.0 mm). However, after cibenzoline had been administered it was similar for both the measured and surrogate data (7 to 8 mm). In the correlation maps of the linearized redundancy $I_\mathrm{m}[s]$ (right column) the short axis length was 8.2 mm and did not change much after infusion of cibenzoline. The long axis length increased from 17.2 mm during sustained AF to 22.9 mm (CIB25–85). Thus, in the left atrium, the short and long axis length estimated from $I_\mathrm{m}[o]$ were somewhat larger than estimated from $I_\mathrm{m}[s]$.

In the left atrium, the short axis length of the linear cross correlation C_0 remained close to control (13.8 mm), while the long axis exceeded the border of the mapped area after drug infusion (Fig. 8, left column). The short axis length of C_m (right column) did not notably increase and remained close to control (23.8 mm). The long axis exceeded the border of the mapped area during the entire experiment.

The average results for all goats are shown in Table 1. In the left atrium, the average

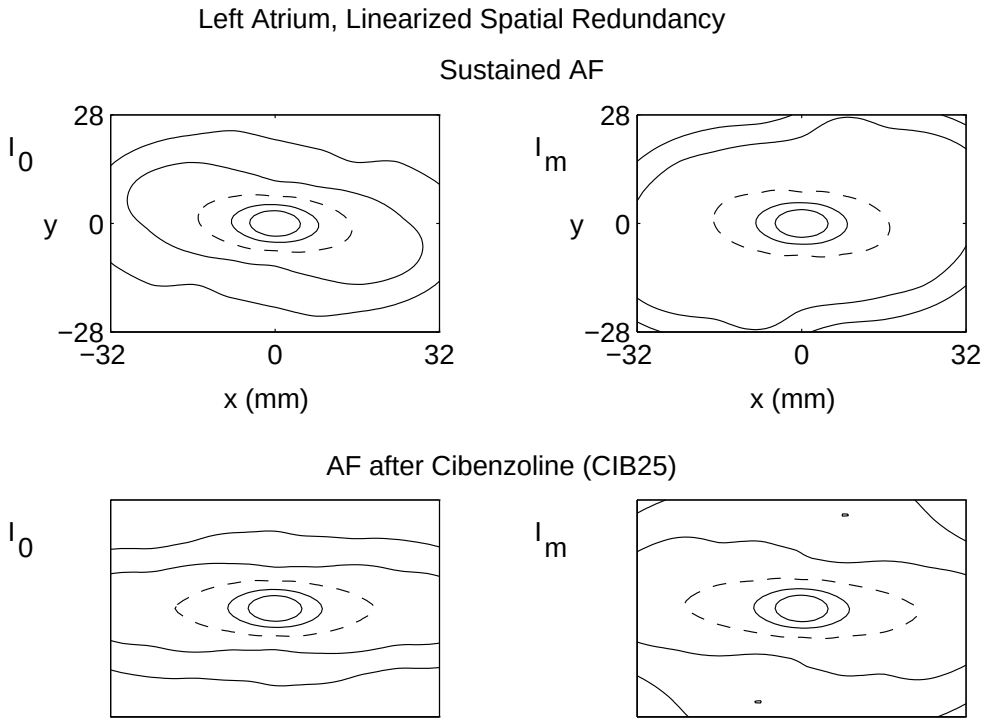

Figure 7: Left atrial correlation maps of the linearized spatial redundancy I_0 (left column) and I_m (right column) during sustained atrial fibrillation (AF) and shortly after infusion of cibenzoline (CIB25). The short axis correlation length of the e^{-1} contour was about 7 mm for both I_0 and I_m both during control and at CIB25. The long axis length somewhat increased from 15.1 to 19.5 mm (I_0) and from 17.2 to 22.9 mm (I_m) after drug infusion.

association length estimated from $I_0[o]$ was 8.2 ± 3.6 mm and remained close to control (7–8 mm) after administration of the drug, with a minor decrease (-12%) noted at CIB50. For the linearized redundancy $I_0[s]$, an increase in association length was observed from 5.1 ± 1.6 mm to 6.4 ± 1.1 mm (CIB85, +26%). The association length estimated from $I_\mathrm{m}[o]$ increased from 9.2 ± 4.1 mm to 12.1 ± 2.4 mm at CIB85 (+32%). For the linearized redundancy $I_\mathrm{m}[s]$, the association length changed from 6.4 ± 2.3 mm to 8.3 ± 1.1 mm (CIB85, +30%). No statistically significant differences were found for the different types of redundancies in the left atrium.

DISCUSSION

Nonlinearity in Activation Patterns of Atrial Fibrillation

We will now discuss the features of the correlation measures presented in Fig. 2 in more detail. The negative values in the linear correlation function C_0 at increasing distance from the reference site (Fig. 2, upper right panel) appeared to be the result from anti–correlation of activation complexes measured simultaneously at different electrode sites: this occurs when a wave is moving away from one electrode (decrease of the action potential to the baseline), but is at the same time sensed as incoming (upstroke of the activation potential) at another electrode. Since the redundancy does not discriminate between positive and negative correlation, this appeared in the nonlinear measure as a positive value for I_0 with increasing electrode distance (Fig. 2,

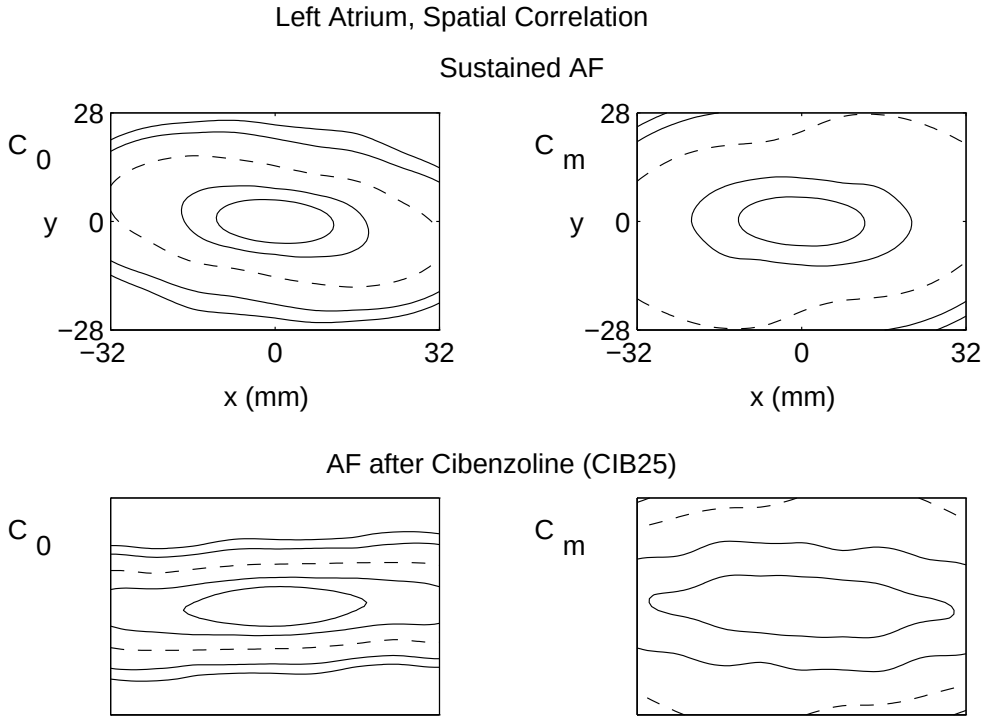

Figure 8: Left atrial correlation maps of the spatial correlation C_0 (left column) and C_m (right column) during sustained atrial fibrillation (AF) and shortly after infusion of cibenzoline (CIB25). The short axis correlation length of the e^{-1} contour of C_0 remained close to control (13.8 mm), while the long axis exceeded the border of the mapped area. The short axis length of C_m (23.8 mm) did not increase and the long axis exceeded the border of the mapped area during the entire experiment.

upper left panel). However, in the linearized redundancy (lower left panel) a peak at $\tau = 0$ was not observed with increasing electrode distance. This means that the peak in I_0 was caused by a predominant nonlinear component, which outweighed the linear correlation. This is understood from the stochastic morphology of the surrogate electrograms (Fig. 1, right panel): contributions to spatial anti–correlation introduced by the shape of activation complexes did not occur anymore since the phase randomization procedure destroyed the characteristic structure of these complexes in each surrogate signal.

Both linear (C_m) and nonlinear (I_m) correlation measures were sensitive to aspects of wave propagation during sustained AF. A peak was present at the delay τ_max, corresponding to the conduction time for propagating activation waves to travel the distance between the recording electrodes. However, this feature of spatial correlation was predominantly a nonlinear aspect of wave propagation since the peak value I_m in the redundancy estimated from the original data was substantially larger than the corresponding peak in the redundancy of the surrogate data.

Summarizing, nonlinearity plays a significant role in the spatio–temporal dynamics of AF when the activation pattern is characterized by single, broad fibrillation waves propagating without substantial conduction delay (AF type I). We note that in a nonlinear analysis of local electrograms of short–lasting, self–terminating atrial fibrillation in humans (Hoekstra et al., 1995), low–dimensional features were identified in patients for which the AF activation pattern was classified as type I. Since nonlinearity is a prerequisite for low–dimensional features, this is

consistent with the observations reported here.

In a recent high–density mapping study the activation patterns during acute and chronic atrial fibrillation in the goat were compared (Konings, 1999). Activation maps of sustained AF were characterized as type III, whereas during short–lasting, acute AF the overall type of fibrillation was less complex (type I). The configuration of unipolar epicardial electrograms during sustained AF showed a high percentage of single potentials (82%, versus 95% during acute AF) with an increased percentage of abnormal beats containing long–double and fragmented potentials (18%, versus 5% during acute AF). Since single potentials were still in the majority during sustained AF, activation was locally fairly homogeneous and many sites were activated by fast and uniformly conducting fibrillation wavelets. It is probably the presence of extended uniformly conducting fibrillation waves (AF type I) which introduces the nonlinearity detected in the spatial correlation analysis of sustained AF (Hoekstra et al., 2000).

However, it is likely that the increased proportion of abnormal electrograms, representing arcs of conduction block, slow conduction or wavelet pivoting (Konings et al., 1997) prevented the manifestation of low–dimensional features characteristic of AF type I in the nonlinear analysis of single, local electrograms of sustained AF which was characterized as type II (Hoekstra et al., 1997).

The different characterization of sustained AF by high–density mapping (type III) and nonlinear time series analysis (type II) might be explained by several factors. First, there was a difference in the total duration of AF, including the time interval that AF was artificially maintained by a pacemaker to induce chronic AF (about 4 to 5 weeks). The seven goats in which high–dimensional mapping experiments were performed during chronic AF had been fibrillating on the average for 142 $\pm$ 55 days (Konings, 1999), while this was 86 $\pm$ 49 days for the five goats used in the nonlinear analysis of sustained AF. Second, the time window for analysis was twelve seconds in the mapping study while recordings of one minute duration were used in the nonlinear analysis of sustained AF. It cannot be excluded that temporal variations among the three types of fibrillation may lead to a different characterization of AF using different time window lengths for the analysis. Furthermore, no pharmacological experiments were performed between mapping of electrically induced AF (type I) during implantation of atrial epicardial electrodes and of chronic AF (type III) during sacrificing of the goats. Instead, a variety of different types of drugs had been administered to the goats in a number of experiments prior to the recording of the episodes of sustained AF used in the nonlinear analysis and it is unknown if these pharmacological experiments affected the dynamics of sustained AF. Finally, although the overall type of fibrillation changed from type I during acute AF to type III during chronic AF, in the acute setting some goats (2 out of 7) exhibited type II fibrillation and in the chronic state some goats (2 out of 7) still had type II (Konings, 1999).

Effects of Cibenzoline on Spatial Organization of AF

The redundancy I_0 characterizes spatial correlation resulting from simultaneous events, and is insensitive to coherence by a mere time delay between signals. Nevertheless, in the right atrium the average short axis association length estimated from I_0 increased shortly after infusion of

cibenzoline (CIB25, +43%) and exceeded the control value over 30% throughout the experiment (Table 1). The nonlinear measure I_{m} accounts for correlation resulting from similar events taking place at different sites yet occurring at a different time. Thus, I_{m} may be considered as an indicator of overall organization, including the effects of wave propagation. A relative increase of 61% (CIB25) to 89% (CIB85) in the average association length estimated from I_{m} was noted in the right atrium. This supports results put forward by the nonlinear analysis applied to single, local electrograms in the same population of goats (Hoekstra et al., 1997) which suggested that cibenzoline increased the degree of organization of atrial activation patterns. In three out of five goats scaling regions appeared in correlation integrals of local atrial electrograms shortly after infusion of cibenzoline and low–dimensional features persisted with increasing dose of cibenzoline. The estimated correlation dimension ($D \simeq 3$ to 4.5) and entropy ($K \simeq 3$ to 6 nats/s) suggested that predominantly single, broad fibrillation waves were activating the mapped area. Therefore, in the right atrium AF was probably maintained by only a few extended macro–reentrant circuits after modification by cibenzoline (AF type I), whereas sustained AF in these same goats during control was characterized as type II by a nonlinear analysis of both single and multiple electrograms, see (Hoekstra et al., 1997) and (Hoekstra et al., 2000), respectively.

The relative effects of cibenzoline on the association length were larger in the right atrium than in the left atrium (Table 1). For instance, the average association length estimated from I_0 in the left atrium slightly decreased after drug infusion (-1 to -12%), whereas in the right atrium an increase of 31 to 43% was observed. Also, the relative increase in short axis association length estimated from I_{m} was 89% at CIB85 in the right atrium, while in the left atrium the increase was limited to 32%. This is consistent with results reported by Hoekstra et al. (1997), where the effects of cibenzoline on the nonlinear parameters seemed to be more pronounced in the right atrium. In particular, the complexity of sustained AF was reduced when the fibrillation rate was still high. The coarse–grained correlation dimension went through a minimum at CIB25 and the coarse–grained correlation entropy adjusted for the changing rate of AF indicated a higher degree of regularity in the morphology of the electrograms. Also, a test for time reversibility suggested that the configuration of AF electrograms became increasingly uniform, containing a higher percentage of (irreversible) single potentials characteristic of rapidly propagating wavefronts in the absence of a large amount of conduction block. The enhanced right atrial spatial organization observed from the spatial correlation analysis is consistent with these dynamical characteristics observed from the nonlinear characteristics of single electrograms.

A difference in the right and left atrial mechanism of activation was also observed by Brugada et al. (Brugada et al., 1993) who performed intra–operative mapping in a patient with chronic atrial fibrillation. Epicardial mapping of both atria showed that multiple wavelets present during AF fused into a single broad wavefront circulating around the right atrial caval veins shortly after administering cibenzoline. The left atrium acted as a bystander and was activated from different sites by wavelets originating from the right atrium. The configuration of atrial electrograms changed from an irregular polymorphic tachycardia into a regular monomorphic arrhythmia after infusion of the drug and it was concluded that cibenzoline transformed random reentry into ordered reentry in the atria.

In a previous study (Hoekstra et al., 2000) the size of a coherent patch of atrial tissue was

estimated as the surface of association spanned by the short and long principal axis of the spatial redundancy I_{m}. This area was used to estimate the number of independent wavelets present in the atria during sustained AF, and the results suggested that on average about one to two wavelets were present under the mapping electrode consistent with type II of AF. Also, it was suggested that larger association lengths result from fewer and larger reentrant circuits. The results presented here support this hypothesis, since the increase of association length was consistent with observations from epicardial mapping studies of atrial activation during vagally induced sustained AF after administration of class IC drugs like flecainide, propafenone and pilsicainide (Iwasa et al., 1998; Wang et al., 1993; Wang et al., 1992). These electrophysiological studies revealed an increase in size and a reduction of the number of reentrant circuits shortly after the start of drug infusion and it was observed that random reentry (AF type II–III) changed into a more organized type of AF (type I).

The pronounced right atrial change of the association length at CIB25 estimated from I_0 (43%) and I_{m} (61%) was less marked for the corresponding linearized redundancies (7% and 23%, respectively). This is attributed to nonlinearity present in the spatial coupling of atrial regions after modification of sustained AF by cibenzoline (characterized as type I) which made the nonlinear correlation measures more sensitive to changes in organization. We note that linear correlation measures have previously been used to characterize changes in spatial organization caused by drug administration. For example, an increase in correlation length by the class IA drug procainamide was reported during AF in patients using a linear correlation function similar to C_{m} (Botteron and Smith, 1995). However, in the present study drug–induced nonlinearity outweighed the linear contribution to spatial organization and therefore nonlinear correlation measures are more effective to characterize changes in spatial coherence of sustained AF during pharmacological intervention with cibenzoline.

Extensive Chaos in the Heart

It is generally believed that for spatially extended systems the dimension and entropy increase linearly with the system size, see e.g. (Chaté, 1995; Grassberger, 1989; Hohenberg and Shraiman, 1989; Torcini et al., 1991). These systems are termed extensively chaotic (Cross and Hohenberg, 1993; Egolf and Greenside, 1994), and it is conjectured that the fractal dimension is related to the system size L as

$$D = \left(\frac{L}{\xi_C}\right)^d \tag{1}$$

for "large" systems with $L \gg \xi_C$, where ξ_C is the "chaos correlation length" and d is the physical dimension. Parts of the system may be considered dynamically independent if they are separated by a distance of order ξ_C. The system then consists of weakly interacting volumes $(\xi_C)^d$, each of which contributes separately to the overall dimension. Currently, it is an important topic in the theory of nonlinear dynamics and pattern formation to connect the chaos correlation length, which determines the length over which the dynamics is physically correlated, to an observable pattern correlation length (Cross and Hohenberg, 1993; Greenside, 1995). If their interrelation can be established, it is possible to estimate the dimension of a large system exhibiting spatio–temporal chaos using Eq. (1), offering an alternative to nonlinear time series methods.

On the basis of correlation length reported (Bayly et al., 1993) and according to the model of extensive chaos Eq. (1), the fractal dimension of VF is about 70, which was used as an estimate of the number of independent surface waves during fibrillation (Egolf and Greenside, 1994). It was argued (Bayly et al., 1993; Egolf and Greenside, 1994) that the existence of many independent regions could explain the lack of evidence for low–dimensional dynamics during VF using dimension estimates (Kaplan and Cohen, 1990a; Kaplan and Cohen, 1990b). However, in a number of numerical studies which use characteristics of spatio–temporal chaos a relation between the correlation length and ξ_C was not found (Egolf and Greenside, 1994; O'Hern et al., 1996).

Infusion of cibenzoline increased the association length during AF and according to Eq. (1) the correlation dimension should decrease, substituting the association length for ξ_C. A decrease of the correlation dimension was indeed reported by Hoekstra et al. (1997) where low–dimensional features were introduced and persisted in the AF dynamics of locally recorded electrograms in goats after administration of cibenzoline. Since the same population of five goats was used in this study, this allows us to relate the results of the spatial correlation analysis presented here to complexity parameters like the (coarse–grained) correlation dimension and entropy which were estimated from single, local electrograms at the same resolution $r = \sigma$ (relative standard deviation) in reconstructed phase space. Assuming Eq. (1) holds, we can give an estimate of ξ_C during AF after cibenzoline was applied. Using a correlation dimension D of about 4 (Hoekstra et al., 1997), and taking the atrial surface in the goat equal to 45 cm^2, the area of coherence is about $\pi\xi_C^2 \simeq 11$ cm^2. This corresponds to a correlation length ξ_C of 1.9 cm, which is of the same order of magnitude as the association length estimated from the spatial redundancy after cibenzoline infusion (Table 1).

Interestingly, recent numerical studies of spatio–temporal chaotic systems exhibiting multiple spiral waves suggest that the average dimension per spiral defect (rotor) is limited (Egolf, 1998). For instance, in a simulation of a two–dimensional excitable medium a mean dimension per reentrant wave of about three to seven was characteristic for a state of fully developed spatio–temporal chaos (Strain and Greenside, 1997). This suggests that only a few fibrillation wavefronts would already be sufficient to generate high–dimensional dynamics at the epicardium, which is in agreement with recent findings in an experimental model of ventricular fibrillation in the isolated rabbit heart (Gray et al., 1995). According to these observations, the low–dimensional features ($D \simeq 3$–4.5, $K \simeq 3$–6 nats/s) observed after drug infusion (Hoekstra et al., 1997) may be associated with the existence of local macro–reentrant circuits during AF. This is consistent with our estimates based on the association length, which indicate that atrial fibrillation was maintained by only a few extended circuits after administering cibenzoline. It may also explain the lack of scaling in correlation integrals of local electrograms recorded during sustained AF (type II), since activation of the mapping electrode by two independent fibrillation waves would already imply a dimension of about six to fourteen. A correlation dimension larger than six is not likely to be identified from experimental time series, regarding the current limitations of dimension algorithms (Eckmann and Ruelle, 1992).

The interpretation of the chaos correlation length is presently not well understood and its relation to different types of correlation lengths is a matter of current investigation (Egolf and

Greenside, 1995; Greenside, 1995; O'Hern et al., 1996; Strain and Greenside, 1997; Zoldi and Greenside, 1997). The association length may be an interesting candidate linking physiological coherence observed in space–time patterns of cardiac fibrillation to the underlying dynamics. Further investigation is required to explore if the model of extensive chaos is applicable to fibrillatory cardiac dynamics, and it remains a challenge how to connect experimental measures of spatial coherence to the chaos correlation length.

Anti–Arrhythmic Mechanisms of Class I Drugs

In normal myocardium the wavelength of atrial tissue is an important marker of both the stability and inducibility of atrial fibrillation (Rensma et al., 1988). A short wavelength in atrial tissue corresponds to conditions which favor AF since the size of reentrant circuits can be small and the tissue mass required for reentry is less. Prolongation of the wavelength would increase the minimum pathlength of reentry and thus reduce the number of functional reentrant waves present in the atria. Under these circumstances the probability that wavelets die out is high leading to termination of AF. If the wavelength exceeds a critical value (about 8 cm in dogs) the atria are not susceptible to AF and reentry can not be induced (Rensma et al., 1988).

Previous electrophysiological studies have shown that class IC drugs show little effect on wavelength, because of the counteracting, balanced effects of slowing conduction and prolonged refractoriness induced by these drugs (Kirchhof et al., 1991). Thus, the concept that a prolongation of the wavelength is anti–arrhythmic appears to be invalidated by the efficacy of class IC drugs to convert AF. Although this seems paradoxical (Allessie and Kirchhof, 1992; Nattel et al., 1997), it should be kept in mind that wavelength is often determined during incremental pacing, while a drug should exert its effects during the very short cycle lengths of fibrillation. It was found that the tachycardia–dependent effect on refractoriness of class IC drugs caused an increase of the refractory period which outweighed the depression in conduction velocity and it was argued that the antifibrillatory action of class IC drugs is based on the ability to increase the wavelength at very rapid rates as found during fibrillation (Kirchhof et al., 1991). These observations were confirmed by mapping studies by Nattel and co–workers (Wang et al., 1992; Wang et al., 1993) who concluded that the anti–fibrillatory action of class I drugs in a model of vagally induced AF in dogs was primarily based on prolongation of the wavelength at rapid rates resulting in an increase of the size and a decrease of the number of reentrant circuits, which increased the chance that AF would terminate.

In a study on the effects of the recently developed class IC drug pilsicainide, this drug was found to be more effective to terminate vagally induced AF in dogs than propafenone, despite a greater effect on the wavelength by propafenone (Iwasa et al., 1998). Furthermore, in the goat model of chronic AF class I drugs cardioverted AF without significant prolongation of the wavelength (Wijffels, 1996; Allessie et al., 1998) and directly after cardioversion the wavelength was still very short as a result of the short atrial refractory period by the AF–induced electrical remodeling of the atria and the depressed intra–atrial conduction after drug administration. As a result atrial vulnerability was still very high and AF could easily be reinduced. These findings point out that the use of the wavelength alone as a parameter to explain the anti–arrhythmic

effects of class I drugs is not fully satisfactory.

Recently, a new hypothesis was put forward to explain the antifibrillatory action of class I drugs. Measurement of the refractory period during atrial fibrillation in the goat model of sustained AF showed that the observed AF cycle length prolongation after drug infusion was primarily due to an increase in the excitable period, and not to lengthening of the functional refractory period (Allessie et al., 1998). This may be caused by a preferential conduction delay at pivot points during reentry so that wavelets are forced to make wider U–turns (lowering of the safety factor for conduction). A widening of the excitable period is thought to be antifibrillatory, since the chance that a wavelet will encounter refractory tissue gets smaller. This would prevent fractionation of reentering wavefronts and thus the genesis of new wavelets.

The increase in spatial coherence caused by cibenzoline may be interpreted as a stabilization of the AF activation pattern, which seems contradictory to the efficacy of this drug in converting AF into sinus rhythm. However, increasing the association length in atria of fixed size is equivalent to keeping the association length fixed and reduce the atrial tissue mass. In both of these cases the atria would look effectively smaller for a given number of reentering fibrillation waves, identifying a coherent patch of tissue with roughly the size of a reentrant circuit. Since it is known that fibrillation is more difficult to sustain in smaller hearts, we conclude that increasing the association length will destabilize atrial fibrillation.

Termination of Atrial Fibrillation

In this study, it was shown that cibenzoline enhanced spatial organization and the space–time pattern of AF seemed rather persistent against intervention by this anti–fibrillatory drug. Thus, it is not clear which mechanism triggered the conversion to sinus rhythm. The main effect of cibenzoline is a reduction of the excitability of myocardial cells. This imposes a source–sink mismatch of electrical excitatory current in reentrant wavefronts (decreased safety factor of wave propagation) causing slow conduction and a decreased curvature of circulating fibrillation waves (Allessie et al., 1998). It is known from the mathematical modeling of excitable media that during conditions of marginal excitability reentry is dominated by the effects of curvature (Fast and Kléber, 1997; Winfree, 1993). It was suggested by Hoekstra et al. (1997) that termination of AF may be triggered when curvature is suppressed to such an extent that the end of wavefronts cannot curl anymore. Consequently, the tip of a reentering wavefront starts to retract (Davydov et al., 1991; Mikhailov and Zykov, 1991) causing decremental propagation and failure of reentry (cf. (Jalife et al., 1996) where this was termed lateral instability of wavebreaks). These critical events would occur in a short time window, just before the termination of AF. However, under these circumstances steady wave propagation would still be viable (Mikhailov and Zykov, 1991; Winfree, 1991) and the sinoatrial node takes over cardiac excitation restoring sinus rhythm. A nonlinear analysis of local AF electrograms revealed that, apart from a reinforcement of spatial organization, the dynamics of sustained AF was not substantially modified by cibenzoline (Hoekstra et al., 1997). The sudden qualitative change in dynamical behaviour at cardioversion suggested that the termination of sustained AF was mediated through a bifurcation of the dynamics.

Conclusions

We studied the effects of the class IC drug cibenzoline on spatial organization in an experimental model of sustained AF and it was shown that this drug exerted substantial effects on both the correlation and association length. In particular in the right atrium, the spatial redundancy (I_{m}) indicated that the association length increased already significantly shortly after the start of infusion (CIB25, 61%), and remained different from control during the experiment. The short axis association length had almost become twice as long with respect to control (increase from 16 to 29 mm at CIB85, 89%), while in the left atrium changes were less pronounced (increase from 9 to 12 mm, 32%). The linearized association length increased more gradually and was less sensitive to changes in spatial organization. Thus, nonlinear correlation measures seem particularly suited to characterize changes in the spatial organization of atrial fibrillation induced by cibenzoline.

The results of the spatial correlation analysis support observations from high–density mapping studies which demonstrated that class IC drugs enhanced the degree of spatial organization in atrial activation patterns of sustained AF at rapid atrial rates, leading to fewer and larger reentrant circuits. The results are also consistent with the dynamical characteristics from a nonlinear analysis of local electrograms (Hoekstra et al., 1997) which suggested that atrial reentry during sustained AF changed from type II to I during experiments to terminate AF with cibenzoline. When the surface spanned by the short and long axis association length is interpreted as the size of a coherent patch of atrial tissue, an increase in association length is equivalent to a reduction of atrial tissue mass available for reentrant circuits. Since fibrillation is more difficult to sustain in smaller atria, the enhanced spatial organization by cibenzoline would destabilize the perpetuation of the arrhythmia.

Theoretic studies of excitable media have revealed that the effects of curvature play an important role under conditions of diminished atrial excitability, which is a characteristic effect of class IC agents. The enhanced spatial organization associated with the observed increase of association length in activation patterns of sustained AF would be a consequence of the chemically induced diminution of curvature of propagating wavefronts. This results in a gradual widening of the paths along which wavelets travel through the atria, leading to termination of AF when curvature is suppressed to such an extent that wavefronts cannot curl any more, preventing the genesis of new wavelets. Recent electrophysiological experiments in the model of chronic AF in goats suggest that the efficacy of cibenzoline to terminate sustained AF is not the result of prolongation of the wavelength of atrial reentry, but rather is an effect of reduced curvature of reentrant activation wavefronts.

With respect to the development of anti–arrhythmic drugs it is important whether the changes observed in the activation pattern of fibrillation can be understood in terms of macroscopic properties using e.g. “generic” models of excitable media, as opposed to detailed ionic models. The detailed study of the kinetics of ionic channels has greatly advanced the knowledge of alterations needed at the cellular level to counter the conditions which initiate and sustain reentry. This has led to the development of anti–arrhythmic agents effective in treating both atrial and ventricular tachyarrhythmias (Breithardt et al., 1995; Camm et al., 1991; Grant,

1997; Rosen, 1995). Despite the success of pharmacological management, the design of drugs is hampered by the difficulty of distinguishing anti–arrhythmic effects from unwanted side effects. For instance, adverse effects like pro–arrhythmia have recently been recognized in clinical drug trials (Epstein et al., 1993).

To appreciate the full bearing of pharmacological intervention it might be worthwhile to explore a reverse strategy: to relate the dynamics observed in macroscopic space–time patterns to alterations in ionic currents and cellular properties that underlie changes at the microscopic level leading to the development of fibrillation. This approach has been advocated by Starmer and coworkers (Starmer et al., 1991; Starmer et al., 1995; Starmer, 1997) who demonstrated that anti–arrhythmic effects on the single cell level can become pro–arrhythmic at the multicellular level, using mathematical models of cardiac excitation. It was pointed out that changes of macroscopic properties like wave propagation must be carefully considered in the design of anti–fibrillatory drugs. In this respect we have shown that the association length is a sensitive marker of drug–induced changes in the organization of atrial action patterns during sustained AF and that it is a useful measure for studying the spatial scales which are relevant during pharmacological intervention to terminate AF.

ACKNOWLEDGMENT

This study was supported by grant no. 805-06-181 from the Council for Earth and Life Sciences (ALW), which is subsidized by the Netherlands Organization for Scientific Research (NWO).

REFERENCES

Allessie, M. A. (1998): Atrial electrophysiological modeling. Another vicious circle? *J. Cardiovasc. Electrophysiol. 9*: 1378–1393.

Allessie, M. A. and Kirchhof, C. J. H. J. (1992): Termination of atrial fibrillation by class IC antiarrhythmic drugs, a paradox? In Kingma, J. H., van Hemel, N. M., and Lie, K. I., editors, *Atrial fibrillation, a treatable disease?* pp: 59–66. Kluwer Academic Dordrecht.

Allessie, M. A., Wijffels, M. C. E. F., and Dorland, R. (1998): Mechanisms of pharmacological cardioversion of atrial fibrillation by class I drugs. *J. Cardiovasc. Electrophysiol. 9*: S69–S77.

Bayly, P. V., Johnson, E. E., Wolf, P. D., Greenside, H. S., Smith, W. M., and Ideker, R. E. (1993): A quantitative measurement of spatial order in ventricular fibrillation. *J. Cardiovasc. Electrophysiol. 4*: 533–546.

Botteron, G. W. and Smith, J. M. (1995): A technique for measurement of the extent of spatial organization of atrial activation during atrial fibrillation in the intact human heart. *IEEE Trans. Biomed. Eng. 42*: 579–586.

Breithardt, G., Borggrefe, M., Camm, J., and Shenasa, M., editors (1995): *Antiarrhythmic drugs: Mechanisms of antiarrhythmic and proarrhythmic actions* Springer-Verlag Berlin.

Brugada, J., Gürsoy, S., Brugada, P., Atié, J., Guiraudon, G., and Andries, E. (1993): Cibenzoline transforms random re–entry into ordered re–entry in the atria. *Eur. Heart. J. 14*: 267–272.

Camm, A. J., Fozzard, H. A., Janse, M. J., Lazzara, R., Rosen, M. R., and for the task force of the working group on arrhythmias of the European Society of Cardiology, P. J. S. (1991): The Sicilian gambit. A new approach to the classification of antiarrhythmic drugs based on their actions on arrhythmogenic mechanisms. *Circulation 84*: 1831–1851.

Chaté, H. (1995): On the analysis of spatiotemporally chaotic data. *Physica D 86*: 238–247.

Cross, M. C. and Hohenberg, P. C. (1993): Pattern formation outside of equilibrium. *Rev. Mod. Phys. 65*: 851–1112.

Davydov, V. A., Zykov, V. S., and Mihailov, A. S. (1991): Kinematics of autowave structures in excitable media. *Sov. Phys. Usp. 34*: 665–684.

Eckmann, J.-P. and Ruelle, D. (1992): Fundamental limitations for estimating dimensions and Lyapunov exponents in dynamical systems. *Physica D 56*: 185–187.

Egolf, D. A. (1998): The dynamical dimension of defects in spatiotemporal chaos. *Phys. Rev. Lett. 81*: 4120–4123.

Egolf, D. A. and Greenside, H. S. (1994): Relation between fractal dimension and spatial correlation length for extensive chaos. *Nature 369*: 129–131.

Egolf, D. A. and Greenside, H. S. (1995): Characterization of the transition from defect to phase turbulence. *Phys. Rev. Lett. 74*: 1751–1754.

Epstein, A. E., Hallstrom, A. P., Rogers, W. J., Liebson, P. R., Seals, A. A., Anderson, J. L., Cohen, J. D., Capone, R. J., and for the Cardiac Arrhythmia Suppression Trial Investigators, D. G. W. (1993): Mortality following ventricular arrhythmia suppression by encainide, flecainide, and moricizine after myocardial infarction. *J. Am. Med. Assoc. 270*: 2451–2455.

Fast, V. G. and Kléber, A. G. (1997): Role of wavefront curvature in propagation of cardiac impulse. *Cardiovasc. Res. 33*: 258–271.

Grant, A. O. (1997): Mechanisms of action of antiarrhythmic drugs: From ion channel blockage to arrhythmia termination. *Pacing Clin. Electrophysiol. 20*: 432–444.

Grassberger, P. (1989): Information content and predictability of lumped and distributed dynamical systems. *Physica Scripta 40*: 346–353.

Gray, R. A., Jalife, J., Panfilov, A. V., Baxter, W. T., Cabo, C., Davidenko, J. M., and Pertsov, A. M. (1995): Mechanisms of cardiac fibrillation. *Science 270*: 1222–1225.

Greenside, H. S. (1995): Spatiotemporal chaos in large systems: The scaling of complexity with size. *Proc. of the CRM workshop on semi–analytic methods for the Navier–Stokes equations, Montreal, Canada* pp: 1–32.

Hoekstra, B. P. T., Diks, C. G. H., Allessie, M. A., and DeGoede, J. (1995): Nonlinear analysis of epicardial atrial electrograms of electrically induced atrial fibrillation in man. *J. Cardiovasc. Electrophysiol. 6*: 419–440.

Hoekstra, B. P. T., Diks, C. G. H., Allessie, M. A., and DeGoede, J. (1997): Nonlinear analysis of the pharmacological conversion of sustained atrial fibrillation in conscious goats by the class Ic drug cibenzoline. *Chaos 7*: 430–446.

Hoekstra, B. P. T., Diks, C. G. H., Allessie, M. A., and DeGoede, J. (2000): Spatial correlation analysis of atrial activation patterns during sustained atrial fibrillation in conscious goats. *Arch. Physiol. Biochem.*

Hohenberg, P. C. and Shraiman, B. I. (1989): Chaotic behavior of an extended system. *Physica D 37*: 109–115.

Iwasa, A., Okumura, K., Tabuchi, T., Tsuchiya, T., Tsunoda, R., Matsunaga, T., Tayama, S., and Yasue, H. (1998): Effects of pilsicainide and propafenone on vagally induced atrial fibrillation: role of suppressant effect in conductivity. *Eur. J. Pharmacol. 356*: 31–40.

Jalife, J., Gray, R. A., Cabo, C., Davidenko, J. M., and Pertsov, A. M. (1996): Atrial fibrillation: Dynamics of rotors and wavelets In Waldo, A. L. and Touboul, P., editors, *Atrial flutter: Advances in mechanisms and management* pp: 121–134. Futura Armonk, New York.

Kaplan, D. T. and Cohen, R. J. (1990a): Is fibrillation chaos? *Circ. Res. 67*: 886–892.

Kaplan, D. T. and Cohen, R. J. (1990b): Searching for chaos in fibrillation In Jalife, J., editor, *Mathematical approaches to cardiac arrhythmias* volume 591 of *Ann. N. Y. Acad. Sci.* pp: 367–374. New York Acad. Sci. New York.

Kirchhof, C., Wijffels, M., Brugada, J., Planellas, J., and Allessie, M. (1991): Mode of action of a new class Ic drug (ORG 7797) against atrial fibrillation in conscious dogs. *J. Cardiovasc. Pharmacol. 17*: 116–124.

Konings, K. T. S. (1999): *Mapping of electrically induced atrial fibrillation in humans.* PhD thesis Maastricht University, The Netherlands.

Konings, K. T. S., Smeets, J. R. L. M., Penn, O. C., Wellens, H. J. J., and Allessie, M. A. (1997): Configuration of unipolar atrial electrograms during electrically induced atrial fibrillation in humans. *Circulation 95*: 1231–1241.

Mikhailov, A. S. and Zykov, V. S. (1991): Kinematical theory of spiral waves in excitable media: Comparison with numerical simulations. *Physica D 52*: 379–397.

Nattel, S., Bourne, G., and Talajic, M. (1997): Insights into mechanisms of antiarrhythmic drug action from experimental models of atrial fibrillation. *J. Cardiovasc. Electrophysiol. 8*: 469–480.

O'Hern, C. S., Egolf, D. A., and Greenside, H. S. (1996): Lyapunov spectral analysis of a nonequilibrium Ising–like transition. *Phys. Rev. E 53*: 3374–3386.

Pompe, B. (1993): Measuring statistical dependences in a time series. *J. Stat. Phys. 73*: 587–610.

Rensma, P. L., Allessie, M. A., Lammers, W. J. E. P., Bonke, F. I. M., and Schalij, M. J. (1988): Length of excitation wave and susceptibility to reentrant atrial arrhythmias in normal conscious dogs. *Circ. Res. 62*: 395–410.

Rosen, M. R. (1995): Cardiac arrhythmias and antiarrhythmic drugs: Recent advances in our understanding of mechanism. *J. Cardiovasc. Electrophysiol. 6*: 868–879.

Starmer, C. F. (1997): The cardiac vulnerable period and reentrant arrhythmias: Targets of anti– and proarrhythmic processes. *Pacing Clin. Electrophysiol. 20*: 445–454.

Starmer, C. F., Lastra, A. A., Nesterenko, V. V., and Grant, A. O. (1991): Proarrhythmic response to sodium channel blockade. Theoretical model and numerical experiments. *Circulation 84*: 1364–1377.

Starmer, C. F., Romashko, D. N., Reddy, R. S., Zilberter, Y. I., Starobin, J., Grant, A. O., and Krinsky, V. I. (1995): Proarrhythmic response to potassium channel blockade. Numerical studies of polymorphic tachyarrhythmias. *Circulation 92*: 595–605.

Strain, M. C. and Greenside, H. S. (1997): Size–dependent transition to high–dimensional chaotic dynamics in a two–dimensional excitable medium Report SG-1, Dept. of Physics Duke University Durham, NC.

Torcini, A., Politi, A., Puccioni, G. P., and D'Alessandro, G. (1991): Fractal dimension of spatially extended systems. *Physica D 53*: 85–101.

Wang, J., Bourne, G. W., Wang, Z., Villemaire, C., Talajic, M., and Nattel, S. (1993): Comparative mechanisms of antiarrhythmic drug action in experimental atrial fibrillation. Importance of use–dependent effects on refractoriness. *Circulation 88*: 1030–1044.

Wang, Z., Pagé, P., and Nattel, S. (1992): Mechanism of flecainide's antiarrhythmic action in experimental atrial fibrillation. *Circ. Res. 71*: 271–287.

Wijffels, M. C. E. F. (1996): *Atrial fibrillation begets atrial fibrillation. An experimental study in chronically instrumented goats.* PhD thesis Maastricht University Maastricht, The Netherlands.

Wijffels, M. C. E. F., Kirchhof, C. J. H. J., Dorland, R., and Allessie, M. A. (1995): Atrial fibrillation begets atrial fibrillation. A study in awake chronically instrumented goats. *Circulation 92*: 1954–1968.

Winfree, A. T. (1991): Varieties of spiral wave behavior: An experimentalist's approach to the theory of excitable media. *Chaos 1*: 303–334.

Winfree, A. T. (1993): How does ventricular tachycardia decay into ventricular fibrillation? In Shenasa, M., Borggrefe, M., and Breithardt, G., editors, *Cardiac mapping* pp: 655–680. Futura Armonk, New York.

Zoldi, S. M. and Greenside, H. S. (1997): Karhunen–Loève decomposition of extensive chaos. *Phys. Rev. Lett. 78*(9): 1687–1690.